Supporting Information

Stolp et al. 10.1073/pnas.1204322109

SI Materials and Methods

Antibodies and Reagents. Antibodies and reagents were as follows: Purified NA/LE hamster anti-mouse CD3ε (145-2C11), rat anti-mouse CD8a-FITC (53-6.7), rat anti-mouse CD8a-PerCP (53-6.7), rat anti-mouse CD62L-biotin (MEL-14), rat anti-mouse CD90.2-APC (53-2.1) Streptavidin-APC (all BD Biosciences). Rat anti-mouse CD4-APC (PJP6) (Immunotools). Rat anti-mouse/human CD44-Biotin (IM7) (Biolegend; BIOZOL). Rabbit anti-PKCζ (C-20), mouse anti-Lck (3A5) (Santa Cruz Biotechnology). Mouse anti-mouse MHC I-APC (H-2Kb), rat anti-mouse CXCR4-PE (2B11), rat anti-mouse CCR7-APC (4B12), eFluor 670 (eBioscience). Mouse anti-GFP (GFP-20), mouse anti-αtubulin (B-5-1-2), Concanvalin A, poly-L-lysine, fibronectin (Sigma). Alexa Fluor 488 donkey anti-sheep IgG, Alexa Fluor 350 goat anti-rabbit IgG, Alexa Fluor 568 goat anti-rabbit IgG, Alexa Fluor 568 goat anti-mouse IgG. Alexa Fluor 568 goat anti-rat IgG, streptavidin Alexa Fluor 660 conjugate, mouse anti-human transferrin receptor (H68.4), TRITC-conjugated Phallotoxin, CellTracker Orange CMTMR, 5-(and 6)-Carboxyfluorescein diacetate succinimidyl ester (CFSE), CellTracker Blue CMAC (all Invitrogen), sheep anti-Nef (1), rabbit antiphosphorylated cofilin (Ser3; 77G2), and rabbit anti MAPK (ERK1/2) (Cell Signaling, New England Biolabs). Recombinant human IL-2 (Biomol), Mowiol 4–88 (Calbiochem, Merck), Retronectin (TaKaRa Bio, MoBiTec), recombinant murine CCL-21 (Peprotech), recombinant tumor necrosis factor-α (Peprotech). The mouse anti-human NGFR antibody was purified from HB8737 hybridoma (ATCC, LGC Standards) cell supernatant. Briefly, HB8737 cells were grown in IMDM medium, supplemented with 10% FCS IgG low, 100 U/mL penicillin, and 100 μg/mL streptomycin (all Gibco, Invitrogen) until confluence, cleared supernatant was concentrated by centrifugation over Amicon Ultra-15 columns (100 kDa cutoff; Millipore), followed by a second purification over a HiTrap protein G HP column (GE Healthcare). The antibody was titered on transiently pSTITCH-IRESΔNGFR–transfected Jurkat T cells, scoring for NGFR cell surface presentation by flow cytometry.

Plasmids and Plasmid Construction. The expression plasmids for pSTITCH-GFP, pHit60 [murine leukemia virus (MLV)-Gag/Pol] as well as for ecotropic (pHit123) and amphotropic (MLV-A) MLV-Env were kindly provided by Reno Debets (Department of Medical Oncology, Erasmus MC, Rotterdam, The Netherlands). For construction of pSTITCH-Nef_{SF2}.GFP and pSTITCH-Nef_{SF2}F195A.GFP a BamHI restriction site was introduced by quick-change PCR directly in front of the GFP coding sequence, disrupting the *gfp* start codon (pSTITCH-BamHI-GFP). Nef_{SF2} and Nef_{SF2}F195A were PCR-amplified from Nef_{SF2}.GFP and Nef_{SF2}F195A.GFP, respectively (2), with BamHI restriction sites on both ends, lacking a Stop codon. Digested PCR products were ligated into BamHI-linearized pSTITCH-BamHI-GFP. For cloning of pSTITCH-IRESΔNGFR, pSTITCH-Nef_{SF2} IRESΔNGFR and pSTITCH-Nef_{SF2}F195A IRESΔNGFR, a HindIII restriction site was introduced in front and a BamHI restriction site behind *gfp* in pSTITCH-GFP by quick-change PCR (pSTITCH-HindIII-GFP-BamHI). The GFP coding sequence was removed from pSTITCH by digestion with HindIII and BamHI. Nef_{SF2} and Nef_{SF2}F195A were PCR amplified from Nef_{SF2}.GFP and Nef_{SF2}F195A.GFP, respectively, with a HindIII restriction site in the front and an EcoRI restriction site in 5′ end behind a stop codon. The IRESΔNGFR sequence was PCR-amplified from an IRESΔNGFR vector with an EcoRI restriction site in the front and a BamHI restriction site in the end (3). Both PCR fragments were ligated into pSTITCH in parallel. All plasmids were confirmed by sequencing and functionality was verified by transient overexpression in human T-cell lines, followed by standard Nef functional analyses.

Western Blotting. Approximately 1×10^6 sorted, transduced murine T lymphocytes were lysed directly in 2× SDS sample buffer and analyzed on 12% SDS/PAGE. For comparison of Nef expression in HIV-infected primary human lymphocytes and Nef transduced primary murine T lymphocytes, infected and transduced cells were sorted, respectively. Sorted cells were adjusted to 70% infection/transduction efficiency and 1×10^6 total cells were lysed and loaded per lane.

Flow Cytometry Analyses of Cell-Surface Receptors. For flow cytometry analyses, 5×10^5 to 2×10^6 lymphocytes were labeled with the following antibodies diluted in PBS: directly fluorophor-coupled CD4-APC (1:20), MHC I-APC (1:100), CXCR4-PE (1:20), CD90.2-APC (1:100), and CD8a-PerCP (1:100) for 30 min on ice; CCR7-APC (1:20) for 30 min at 37 °C; CD62L-Biotin (1:100) and NGFR (1:800) for 30 min on ice, followed by a washing step in PBS and incubation with the fluorophor-coupled secondary reagent/antibody streptavidin-APC (1:20) and anti-mouse APC (1:250), respectively, for 30 min on ice. Following a washing step in PBS, 5,000 transduced cells were analyzed for cell-surface receptor modulation by flow cytometry. Receptor down-modulation was calculated relative to untransduced cells and GFP-transduced control cells were set to 100% as described previously (2).

Immune Fluorescence Analyses and GTPase Activity Assays. Analysis of the Lck accumulation, chemokine-induced membrane-ruffle formation and cofilin-phosphorylation were essentially performed as described previously (2, 4). Approximately 5×10^5 cells were seeded per poly-L-lysine–coated cover-glass. Next, 200 ng/mL recombinant murine CCL-21 was used to induce F-actin rich membrane ruffle formation. When NGFR-sorted lymphocytes were used, Nef was detected by sheep anti-Nef (1:500) antibody followed by labeling with Alexa Fluor 488 donkey anti-sheep IgG (1:1,000). For analysis of cell polarization, transduced lymphocytes were plated onto fibronectin-coated cover-glasses (10 μg/mL fibronectin for 30 min at 37 °C) and stimulated with 100 ng/mL recombinant murine CCL-21 for 30 min at 37 °C before PFA fixation (3.7% PFA, 15 min, room temperature). Cells were permeabilized with 0.1% triton-X 100 for 2 min, blocked with 1% BSA/PBS for 30 min, and stained with primary antibodies rat anti–CD44-biotin (1:200) and rabbit anti-PKCζ (1:50) for 2 h. Independent stainings were performed for confocal image acquisition and manual counting at a fluorescence microscope. Following PBS wash, CD44 was revealed by either Alexa Fluor 568 goat anti-rat IgG (1:1,000) or streptavidin Alexa Fluor 660 conjugate (1:500), PKCζ with Alexa Fluor 350 goat-anti-rabbit IgG (1:500) or Alexa Fluor 568 goat anti-rabbit IgG (1:1,000). Phenotypes were quantified by manual counting of at least 100 transduced cells per cover glass at an Olympus IX81 microscope with Cell^M software. Confocal stacks of chemokine induced membrane ruffling were obtained with a Leica TCS SP5 microscope and LAS AF software. All other confocal micrographs were acquired using a Zeiss LSM 510 Axiovert microscope and LSM Meta software.

Rac1 activity of transduced and sorted primary murine lymphocytes following chemokine stimulation was analyzed performing a Rac1-GLISA (Cytoskeleton) according to the manufacturers' instructions. Briefly, transduced and sorted lymphocytes were starved for 24 h in medium containing 1% BSA. Before chemokine stimulation, lymphocytes were cultured at 2×10^6 cells/mL in a 37 °C

water-bath for 10 min. Then, 200 ng/mL CCL-21 was added to the cells and stimulation was stopped after 1 and 10 min by transferring the cells into a large volume of ice-cold PBS; 2×10^6 cells were used per sample for triplicate analyses.

Isolation, Culture, and HIV Infection of Human Peripheral Blood Mononuclear Cells. Human peripheral blood mononuclear cells were isolated, stimulated, and infected with HIV, as described previously (2). Proviral constructs and virus production has been described previously (2).

MLV-Based Vector Production. Vector production was optimized regarding use of the vector-producing cell line, transfection reagent, plasmid ratios, pseudotyping of the particles, different GagPol constructs, lentiviral vs. MLV-based vector systems and harvesting time points, resulting in the following vector production protocol (workflow shown in Fig. S1): 293T cells were maintained in DME medium with high glucose, supplemented with 10% FCS, 100 U/mL penicillin, 100 μg/mL streptomycin. Twenty-four hours before transfection, 5×10^6 293T cells were seeded per 15-cm dish. Transfection was performed using JetPEI transfection reagent (Peqlab) according to the manufacturers' recommendations using: 20 μg pSTITCH, 20 μg pHit60, 5 μg pHit123, and 5 μg MLV-A. The transfection mix was directly added to the medium and a medium exchange was performed after 5 h. Virus supernatant was harvested after 48 h or 72 h by filtration of the cell supernatant (0.22-μm pore-size radio-sterilized filters) and used immediately for transduction of primary murine T lymphocytes.

Preparation and Transduction of Murine T Lymphocytes. The preparation and transduction protocol for murine T lymphocytes was optimized with respect to in vitro stimulation (anti-CD3/CD28 vs. ConA/IL-2), culture density during stimulation, duration of mitogenic stimulation before transduction, cell density during transduction, format of transduction (24- to 96-well plates), reagents used to increase transduction efficiency (polybrene vs. retronectin), centrifugation speed, and duration of spin infection, culture density following transduction, timing of dynabead-sorting, and read-out. The optimized protocol is illustrated in Fig. S1. Six- to 9-wk-old WT C57BL/6 mice (Charles River) were kept in the central animal facility of the University Heidelberg and were killed by CO_2 perfusion (approved by the University of Heidelberg G-152/07). Spleen, peripheral, and mesenteric lymph nodes were harvested and single-cell suspensions were maintained by squeezing organs through cell strainers (70 μm; BD Biosciences). After red blood cell lysis, lymphocytes were washed, counted, and cultured at 2×10^6 cells/mL in complete mouse medium (CMM: RPMI 1640 GlutaMAX, supplemented with 15% FCS, 100 U/mL penicillin, 100 μg/mL streptomycin, 2 mM Glutamine, 50 μM 2-mercaptoethanol, 1× nonessential amino acids, 1× sodium pyruvate, 1× MEM vitamins; all from Gibco, Invitrogen) containing 2 μg/mL Concavalin A (ConA; Sigma) and 2×10^5 U/mL recombinant human IL-2 (Biomol). For transduction, 24-well plates were coated with 16 μg/mL retronectin/PBS for 3 h at 37 °C. Retronectin (TaKaRa Bio, MoBiTec) was recycled up to 10 times and stored at −20 °C. Retronectin coated plates were stored in PBS, at 4 °C for up to 2 wk. One day after lymphocyte preparation, 2 mL of fresh filtered virus supernatant per well were spun for 1 h at 4,000 rpm at room temperature onto the retronectin-coated plates. Virus supernatant was removed subsequently and 2 mL of new virus supernatant was added per well together with 2×10^6 lymphocytes. Cells were spin-infected for 1 h at 2,300 rpm at room temperature and cultivated for 5 h at 37 °C 5% CO_2, before performing a medium exchange. Cells were resuspended at 1×10^6 cells/mL in CMM containing 2×10^5 U/mL IL-2. Sorting and experiments were performed 24 or 48 h after transduction, respectively.

Dynabead Sorting of ΔNGFR$^+$ Cells. Twenty-four hours post-transduction, ΔNGFR-transduced cells were sorted using the CELLection Pan Mouse IgG Kit (Invitrogen) according to the manufacturers' recommendations. Briefly, transduction efficiency was analyzed by flow cytometry and 25 μL of Pan Mouse IgG Dynabeads were coupled with 2 μL of the purified hybridoma-derived anti-NGFR antibody (HB8737 hybridoma; ATCC, LGC Standards) per 2.5×10^6 ΔNGFR$^+$ cells for 45 min at 4 °C, rocking. Following extensive washing, total lymphocytes were diluted to 10^7 cells/mL and added to the antibody-coupled beads. After incubation for 30 min at 4 °C, rocking, unbound cells were removed by extensive washing and bound ΔNGFR$^+$ lymphocytes were eluted from the beads by DNase I treatment. This purification protocol yielded 95–99% pure ΔNGFR$^+$ lymphocytes. Cells were either incubated at 1×10^6 cells/mL in CMM containing 2×10^5 U/mL IL-2 for another 24 h at 37 °C and 5% CO_2 before analysis, or used immediately in case of 24-h homing.

Transwell Chemotaxis Assay. The transwell chemotaxis assay was essentially performed as described previously (2), using 50 ng/mL recombinant murine CCL-21 as chemoattractant. Where indicated, transwell inserts with 3-μm pore size (Costar #3415) were used instead of 5 μm (Costar #4321). In the case of NGFR-sorted lymphocytes, input and migrated cells were counted manually using a Neubauer counting chamber and Trypan blue to exclude dead cells, because ~100% of the cells were transduced. Chemotaxis efficiency was calculated relative to the control cells. Usually about 60% of the input cells migrated within the 2 h of the experiment.

The transwell chemotaxis assay toward sphingosine-1-phosphate (S1P) was performed as previsously described (5). Briefly, transduced cells were starved for 24 h in medium containing 1% fatty acid-free BSA (Sigma) before chemotaxis toward 25 nM S1P (Sigma) at 37 °C 5% CO_2 for 4 h.

Live T-Lymphocyte Migration in 3D Fibrillar Collagen. ΔNGFR transduced cells were sorted 24 h posttransduction using the CD271 MicroBead APC Kit (MiltenyiBiotec) according to the manufacturer's instructions. Briefly, 1×10^7 total cells were resuspended in 80 μL MACS buffer (PBS, 2 mM EDTA, 0.5% FCS), 10 μL of FcR Blocking Reagent, and 10 μL of APC-coupled NGFR antibody were added and refrigerated for 10 min. After washing, cells were resuspended in 70 μL MACS buffer, 10 μL FcR Blocking Reagent, and 20 μL of anti-APC MicroBeads were added and refrigerated for 15 min. After washing, cells were positively separated using the autoMACS Pro Seperator (program possel-d). Cells were allowed to rest in CMM for several hours before subjecting them to collagen migration experiments. This procedure yielded between 90% and 98% ΔNGFR$^+$ cells and the experimental performance of cells in collagen matrix was the same as upon sorting using CELLection Pan Mouse IgG Kit (Invitrogen).

Cell migration in 3D collagen I lattices was monitored by time-lapse microscopy within self-constructed migration chambers: A coverslip was connected to an object slide by a dental wax spacer, which was cut into pockets open to one side (approximate chamber size of 8 × 4 x 2 mm, volume of ~120 μL). Through the openings the pockets were partly filled with a collagen matrix including the cells. Cell-containing collagen gels were prepared as described (6): Low-density collagen matrix (1.6 mg/mL) was prepared by mixing 750 μL bovine collagen I (PureCol, Nutacon) with bicarbonate-buffered MEM [50 μL 7.5% $NaHCO_3$ and 100 μL 10× MEM (Gibco)]. One-hundred microliters of matrix were subsequently combined with 50 μL cell-suspension (3×10^6 cells/mL in 0.5% FCS-reduced media) and allowed to polymerize at 37 °C. High-density collagen matrices (4.6 mg/mL) were prepared correspondingly using highly concentrated rat collagen I (BD Biosciences) and the bicarbonate-buffered MEM described above. After polymerization, gels were overlaid with FCS reduced media containing 100 ng/mL CCL-21 (Peprotech) and were sealed with melted dental wax.

The samples were monitored via bright-field of an inverse light microscope (10× objective, Axiovert 200M; Zeiss) coupled to an EM-CCD camera (Roper Scientific), equipped with a climatization control maintaining 37 °C. For the duration of 2.5 h, pictures were taken in 3-min intervals. Cells were scored as migrating if they once left their initial position during the time-lapse monitoring. Migrating cells were then tracked manually using the ImageJ manual tracking plugin and analyzed with the chemotaxis tool plugin. Collagen matrix consistency was visualized by confocal reflection microscopy using the 488-nm laser and 40× oil immersion objective of a Leica TCS SP5 microscope. A 10-μm stack of optical sections (*z*-stack) was acquired in 0.5-μm slices, which were subjected to maximum projections using the LAS AF software.

Homing to Lymphoid Organs. Transduced and NGFR-sorted T lymphocytes were labeled with CellTracker dyes (Invitrogen) at 1×10^7 cells/mL at 37 °C: CMTMR 5 μM 20 min, CFSE 2.5 μM 15 min, eFluor670 2.5 μM 20 min. Dyes were exchanged between samples for successive replicates to exclude effects of the dyes on homing behavior. Subsequently, cells were washed with CMM and resuspended at 1×10^8 cells/mL 5×10^6 IRESΔNGFR control cells were coinjected with an equal number of Nef wt or F195A expressing cells into the retrobulbar sinus of 6- to 8-wk-old WT C57BL/6 mice. Four and 24 h after adoptive transfer spleen, peripheral, and mesenteric lymph nodes were harvested separately and single-cell suspensions were obtained as described above. Cells were either subjected immediately to flow cytometry to analyze the relative abundance of CellTracker-positive cells or labeled with anti-CD90.2 and anti-CD8a antibodies (BD Biosciences) to distinguish between the homing efficiency of $CD4^+$ and $CD8^+$ T lymphocytes. Between 500,000 and 750,000 cells were acquired per sample. Homing ratios of Nef WT or F195A expressing cells were calculated relative to control cells for each organ. All experiments were approved by the Kanton of Bern and comply with kantonal and federal animal experimentation regulations.

Transendothelial Migration Assay, Single-Cell Tracking, and Scanning Electron Microscopy. Primary mouse brain microvascular endothelial cells (pMBMECs) were isolated from sex-matched 5- to 8-wk-old C57BL/6 mice, cultured in DMEM, 20% FCS, 1 mmol/L sodium pyruvate, 1% nonessential amino acids, 50 μg/mL gentamycin, and 1 ng/mL basic fibroblast growth factor (7, 8). pMBMECs were stimulated with TNF-α (25 ng/mL; Peprotech) for 16–18 h. All experiments were performed in migration assay medium (DMEM, 5% calf serum, 25 mM Hepes) at 37 °C.

For live-cell imaging, a parallel flow chamber connected to an automated syringe pump (Harvard Apparatus) was mounted on TNF-α–stimulated pMBMECs previously overlaid with 1 μM CCL-21 and placed on the heating stage of an inverted microscope (AxioObserver Z1; Carl Zeiss). Shear stress (dyn/cm^2) was calculated as previously described (7).

Transduced and NGFR-sorted T lymphocytes (1×10^7 cells/mL) labeled with CellTracker dyes (CMTMR, 5 μM, 15 min, CFSE, 2.5 μM, 10 min and CMAC, 10 μM, 15 min; dyes were exchanged between samples for successive replicates to exclude adverse effects of the dyes) were allowed to accumulate for around 1 min at low shear stress (0.15 dyn/cm^2). Then, dynamic T-lymphocyte interactions with pMBMECs were recorded under physiological shear stress (1.5 dyn/cm^2) using a 20× objective with phase contrast and fluorescence illumination. Time-lapse videos were created from one frame every 20 s.

Adherence to the endothelium was calculated relative to the percentage of each cell population in the input. Cells were tracked manually by the ImageJ manual tracking plugin and analyzed by the chemotaxis tool plugin. Polarization indices of cells while migrating on the endothelium were assessed by manually measuring length and width of single cells using ImageJ and dividing cell length by cell width.

For scanning electron microscopy (SEM), lymphocytes were allowed to interact with the endothelial cells for 5 min before fixation with 2.5% glutaraldehyde overnight. After dehydration with ethanol, samples were critical point dried, followed by overnight drying. Next, samples were sputter-coated with a 10-nm layer of gold and analyzed using SEM to visualize filopodia.

Two-Photon Intravital Microscopy of Popliteal Lymph Nodes. Two-photon intravital microscopy (2PM) was essentially performed as previously described (9). Briefly, transduced and NGFR-sorted T lymphocytes were labeled with CellTracker dyes as described above. Next, 4×10^6 IRESΔNGFR control cells were coinjected with 8×10^6 Nef WT-expressing cells into the retrobulbar sinus of 6- to 8-wk-old WT C57BL/6 mice. One day after adoptive transfer, recipient mice were anesthetized and the right popliteal lymph node was surgically exposed. Before recording, 10 μg Alexa 633-conjugated MECA-79 was injected intravenously to label high endothelial venules (HEV). The 2PM was performed with an Olympus BX50WI fluorescence microscope equipped with a 20× objective and a TrimScope 2PM system controlled by ImSpector software (LaVision Biotec). For two-photon excitation, a Ti:sapphire laser (MaiTai HP) was tuned to 780 nm. For 4D analysis of cell migration, 14–22 *x*-*y* sections with *z*-spacing of 4 μm (300 × 300 × 56–88 μm) were acquired every 20 s for 20 min. Emitted light was detected through 447/55-nm, 525/50-nm, 593/40-nm, and 655/40-nm bandpass filters with nondescanned detectors to generate four-color images. Sequences of image stacks were transformed into volume-rendered 4D videos with Volocity software, which was also used for semiautomated tracking of cell motility in three dimensions. Cellular motility parameters were calculated from *x*, *y*, and *z* coordinates of cell centroids using Volocity and MatLab protocols. The instantaneous 3D velocity is the velocity between two frames. The motility coefficient, a measure of the ability of a cell to move away from its starting position, was calculated from the gradient of a graph of mean displacement against $\sqrt{(\text{time})}$.

Statistical Analysis and Software. Statistical significance on parametrically distributed datasets was calculated performing a Student *t* test (or Mann–Whiteney test for not normally distributed datasets) or a one-tailed ANOVA test with a Newman–Keuls posttest when comparing two or several datasets, respectively ($^{***}P < 0.0005$, $^{**}P < 0.005$, $^{*}P < 0.05$). The nonparametric Kruskal–Wallis test was used for evaluation of the lymph node homing because of the limited available sample size. Calculations were done with Microsoft Excel and GraphPad Prism; image-editing was performed using Adobe Photoshop and Illustrator CS5.

1. Fackler OT, et al. (2006) Functional characterization of HIV-1 Nef mutants in the context of viral infection. *Virology* 351(2):322–339.
2. Stolp B, et al. (2009) HIV-1 Nef interferes with host cell motility by deregulation of Cofilin. *Cell Host Microbe* 6(2):174–186.
3. Abad JL, et al. (2002) Single-step, multiple retroviral transduction of human T cells. *J Gene Med* 4(1):27–37.
4. Haller C, Rauch S, Fackler OT (2007) HIV-1 Nef employs two distinct mechanisms to modulate Lck subcellular localization and TCR induced actin remodeling. *PLoS ONE* 2 (11):e1212.
5. Nombela-Arrieta C, et al. (2007) A central role for DOCK2 during interstitial lymphocyte motility and sphingosine-1-phosphate-mediated egress. *J Exp Med* 204(3): 497–510.
6. Friedl P, Bröcker EB (2004) Reconstructing leukocyte migration in 3D extracellular matrix by time-lapse videomicroscopy and computer-assisted tracking. *Methods Mol Biol* 239:77–90.
7. Steiner O, et al. (2010) Differential roles for endothelial ICAM-1, ICAM-2, and VCAM-1 in shear-resistant T cell arrest, polarization, and directed crawling on blood-brain barrier endothelium. *J Immunol* 185(8):4846–4855.
8. Coisne C, et al. (2005) Mouse syngenic in vitro blood-brain barrier model: A new tool to examine inflammatory events in cerebral endothelium. *Lab Invest* 85(6): 734–746.
9. Boscacci RT, et al. (2010) Comprehensive analysis of lymph node stroma-expressed Ig superfamily members reveals redundant and nonredundant roles for ICAM-1, ICAM-2, and VCAM-1 in lymphocyte homing. *Blood* 116(6):915–925.

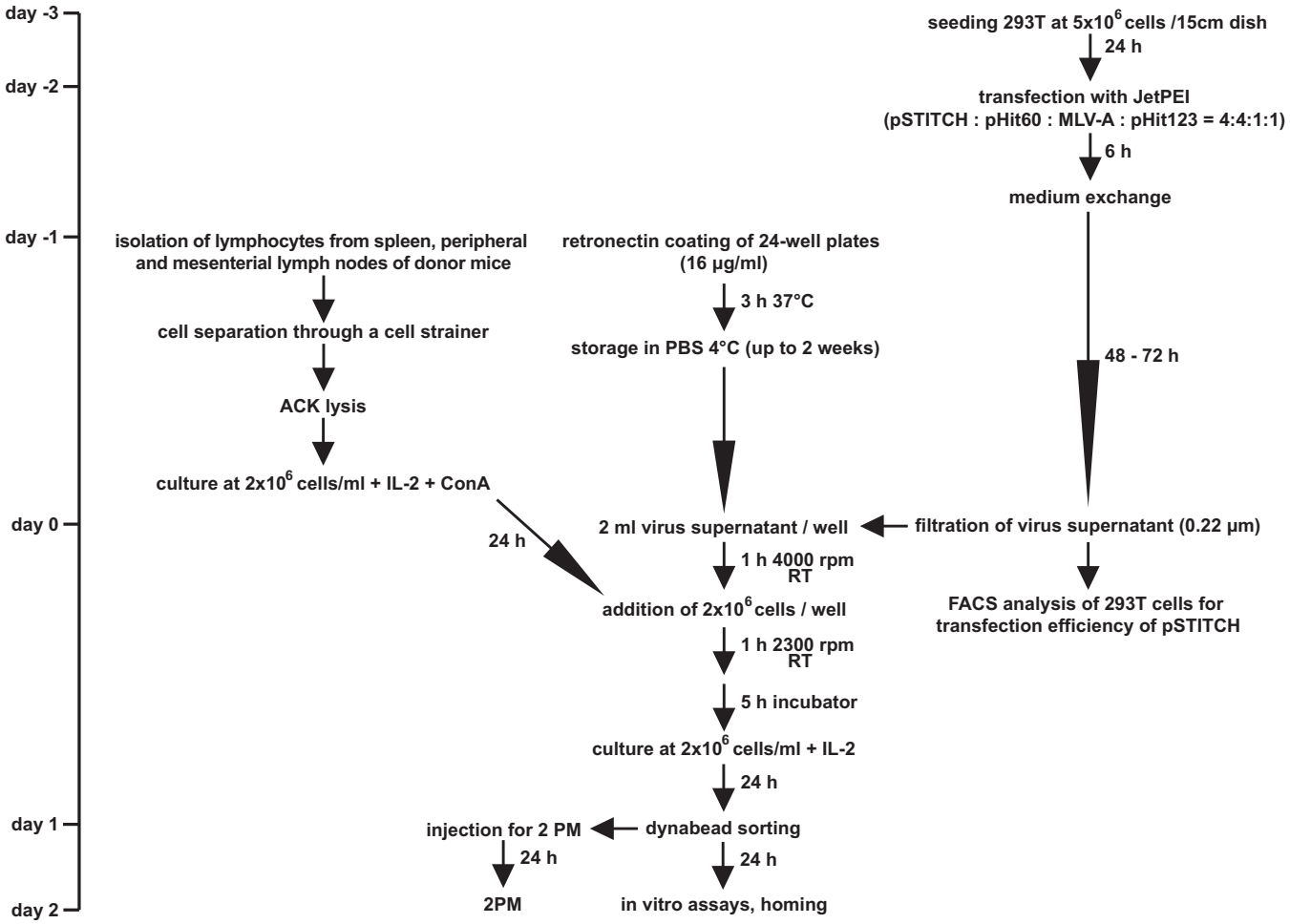

Fig. S1. Scheme of the optimized protocol for efficient transduction of primary murine T lymphocytes.

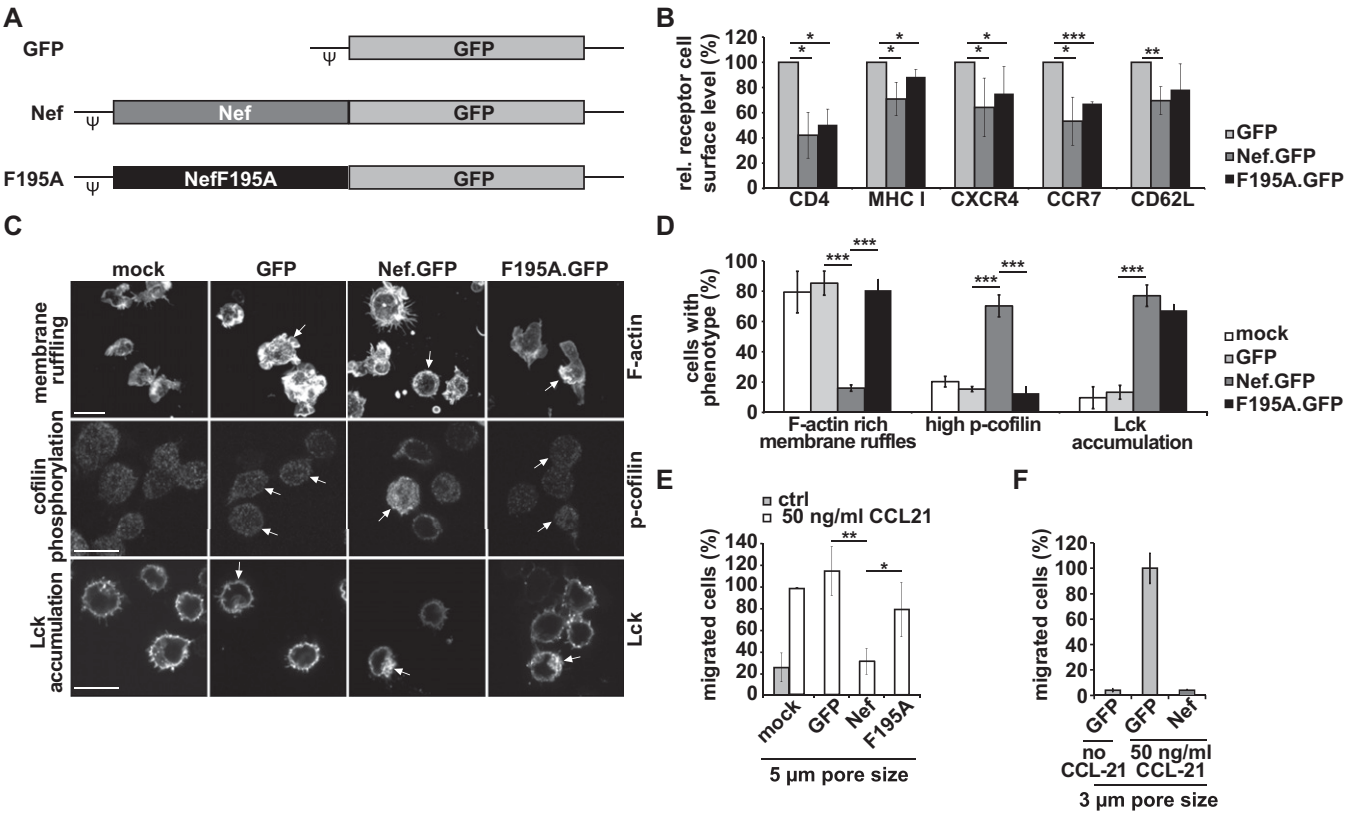

Fig. S2. Nef function is recapitulated in primary murine T lymphocytes. Primary murine T lymphocytes were isolated from spleen and lymph nodes of donor mice, stimulated and retrovirally transduced in vitro, as described in Fig. S1. Analyses were performed 24 h posttransduction. Shown are mean values with SD from three independent experiments. *P* values have been calculated performing a Student *t* test. (*A*) Schematic drawing of the pSTITCH-based packaging constructs used to achieve expression of GFP, Nef.GFP, or NefF195A.GFP in primary murine T lymphocytes. (*B*) Relative receptor down-modulation by Nef of the cell-surface receptors CD4, MHC class I, CXCR4, CCR7, and CD62L. Down-modulation was calculated relative to untransduced control cells in each sample with GFP expressing controls set to 100%. (*C*) Representative confocal micrographs of transduced T lymphocytes plated onto poly-L-lysine–coated cover-glasses. Cells were analyzed for membrane ruffling upon stimulation with 200 ng/mL CCL-21, cofilin phosphorylation, and Lck accumulation, respectively. Cells were fixed and stained for F-actin, phosphorylated cofilin (p-cofilin) or Lck as indicated. Arrows highlight transduced GFP+ cells. (Scale bars, 10 μm.) (*D*) Quantification of the cells shown in *C*. Cells showing F-actin rich membrane ruffles, high p-cofilin levels, or Lck accumulation were quantified by manual counting of at least 100 transduced cells per condition. (*E* and *F*) Analysis of chemotaxis toward CCL-21 in a transwell assay using a membrane with 5 μm (*E*) or 3 μm (*F*) pore size. Migration of transduced cells was calculated relative to GFP-expressing cells. $*P < 0.05$; $**P < 0.005$; $***P < 0.0005$.

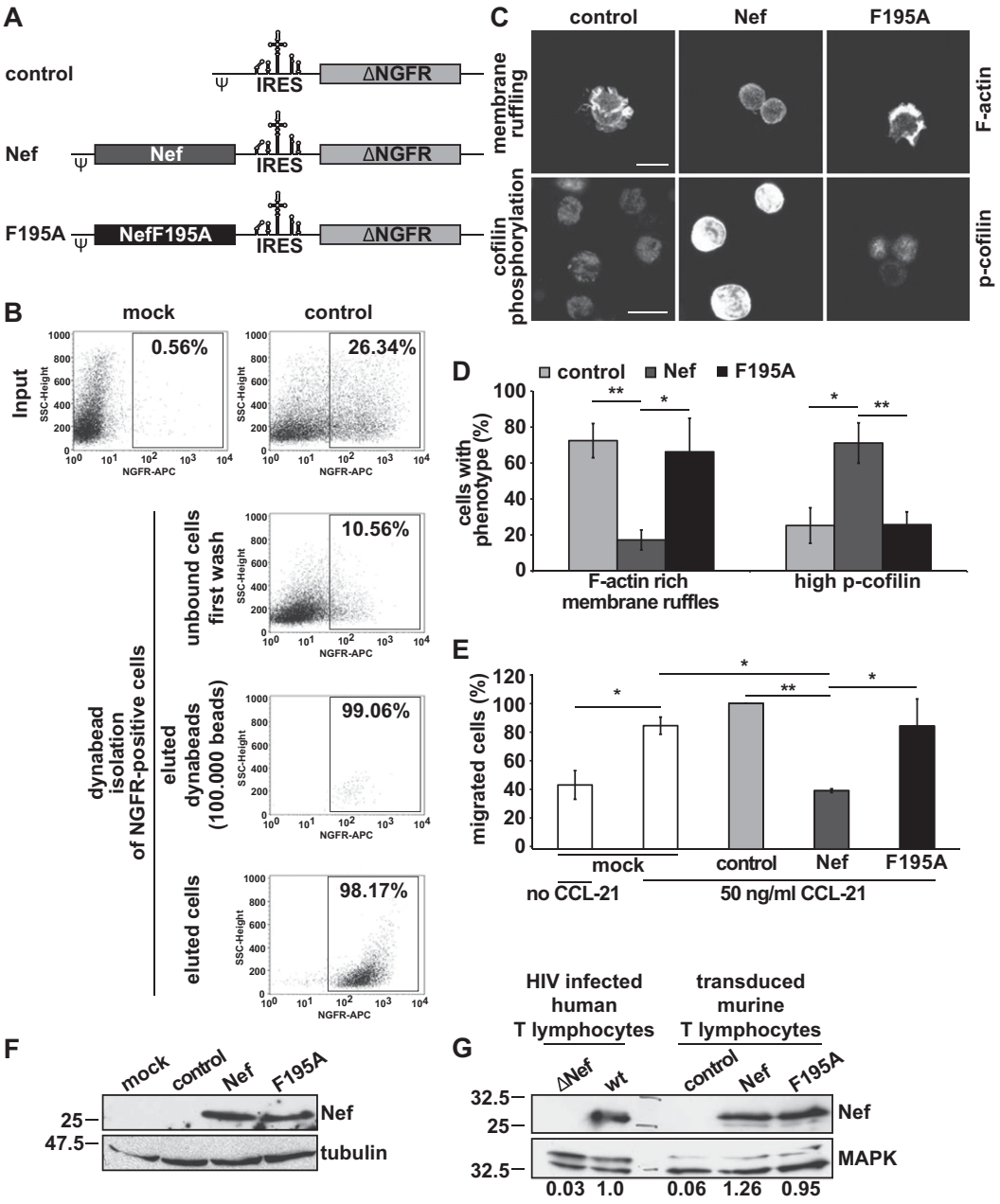

Fig. S3. Sorting of transduced T lymphocytes by their NGFR cell-surface marker results in homogenous cell populations with Nef expression levels and function comparable to HIV-infected primary human T lymphocytes. (*A*) Schematic drawing of the pSTITCH-based packaging constructs used to achieve expression of ΔNGFR alone or together with Nef or its F195A mutant in primary murine T lymphocytes. (*B*) Primary murine T lymphocytes were isolated from spleen and lymph nodes of donor mice, stimulated and retrovirally transduced in vitro as described in Fig. S1. Twenty-four hours posttransduction successfully transduced cells were sorted using dynabeads coated with an anti-NGFR antibody. Shown are transduced cells before (Input) and after (unbound cells first wash) dynabead-dependent depletion of NGFR$^+$ cells as well as DNase I-treated dynabeads (eluted dynabeads) and the obtained pure NGFR$^+$ cell population (eluted cells). The numbers in the gates represent the percentage of NGFR$^+$ T lymphocytes in the sample. Following sorting, T lymphocytes were cultured for another 24 h before analysis. (*C*) Representative confocal micrographs of transduced, sorted T lymphocytes, plated onto poly-L-lysine coated cover-glasses and stimulated with 200 ng/mL CCL-21 to induce membrane ruffling or left untreated for analysis of cofilin phosphorylation. Cells were fixed and stained for F-actin and p-cofilin, as indicated. All cells shown are ΔNGFR$^+$ because of previous sorting. (Scale bars, 10 μm.) (*D*) Quantification of the cells shown in *C* that display F-actin rich membrane ruffles or cofilin hyperphosphorylation, respectively. Shown are mean values with SD of three independent experiments with at least 100 transduced cells manually counted per condition. *P* values have been calculated performing a Student *t* test. (*E*) The cells shown in *C* were subjected to a transwell chemotaxis assay toward CCL-21. Chemotaxis efficiency was calculated relative to control cells. Shown are mean values with SD of three independent experiments. *P* values have been calculated performing a Student *t* test. (*F*) Representative Western blot of the cells shown in *C*, probed for Nef and tubulin as a loading control. (*G*) Western blot of HIV-infected primary human T lymphocytes and primary murine T lymphocytes transduced with the constructs shown in *A*. Infected/transduced cells were enriched and cell populations adjusted to contain 70% infected or transduced cells. Next, 1×10^6 were lysed and subjected to Western blot analysis for expression of Nef and MAPK (loading control). Intensities of the Nef bands was quantified and normalized to the corresponding MAPK signal. Numbers below the panels indicate Nef expression levels relative to that observed in human peripheral blood mononuclear cells infected with HIV-1 WT, which was arbitrarily set to 1. *$P < 0.05$; **$P < 0.005$.

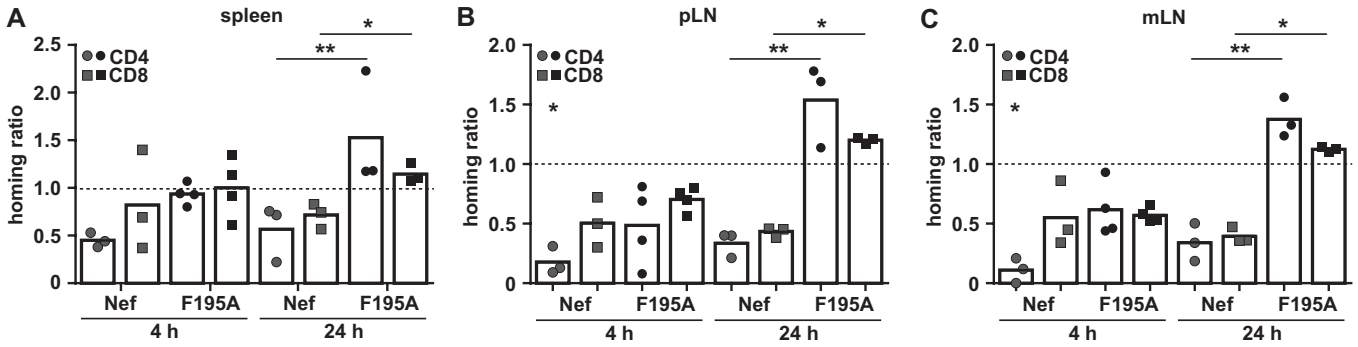

Fig. S4. Nef interferes with T lymphocyte homing to lymph nodes. Primary T lymphocytes were isolated, transduced, and sorted as described in Fig. S3. Cells were labeled with CellTracker dyes and adoptively transferred into recipient mice. Control cells were always coinjected with Nef or F195A-expressing T lymphocytes as an internal control. Spleen (*A*), peripheral (pLN) (*B*), and mesenteric (mLN) (*C*) lymph nodes were harvested after 4 or 24 h and single-cell suspensions were analyzed by flow cytometry following cell surface labeling with anti-CD90.2 and anti-CD8a antibodies to distinguish between $CD4^+$ (round symbols) and $CD8^+$ (square symbols) T lymphocytes. The homing ratio in each mouse was calculated relative to the coinjected control cells that was arbitrarily set to 1. Each symbol represents data observed from one animal. *P* values have been calculated performing a Kruskal–Wallis test with a Dunn's posttest. $*P < 0.05$; $**P < 0.005$.

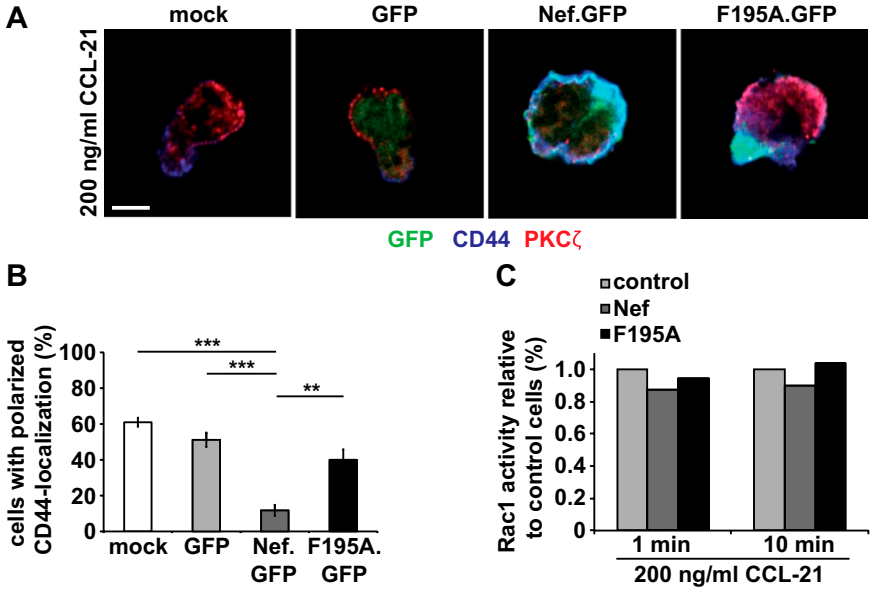

Fig. S5. Nef interferes with T lymphocyte polarization but not Rac1 activity. (*A*) Representative confocal micrographs of primary mouse T lymphocytes expressing GFP, Nef wt.GFP or Nef F195A.GFP following retroviral transduction. Cells were plated onto fibronectin-coated cover-glasses, stimulated with 100 ng/mL CCL-21 for 30 min, fixed, and stained for the trailing edge marker CD44 (blue) and the leading edge marker PKCζ (red). (Scale bar, 10 μm.) (*B*) Quantification of the cells shown in *A* with polarized localization of CD44 to the trailing edge. Shown are mean values with SD of three independent experiments with at least 100 transduced cells manually counted per condition. *P* values have been calculated performing a Student *t* test. (*C*) Primary murine T lymphocytes were transduced with the constructs shown in Fig. S3, sorted based on NGFR expression, and starved for 24 h. Rac1-activity following CCL-21 stimulation for 1 and 10 min was analyzed by a Rac1-GLISA. Shown are the mean values of triplicate measurements of one representative of two experiments. $**P < 0.005$; $***P < 0.0005$.

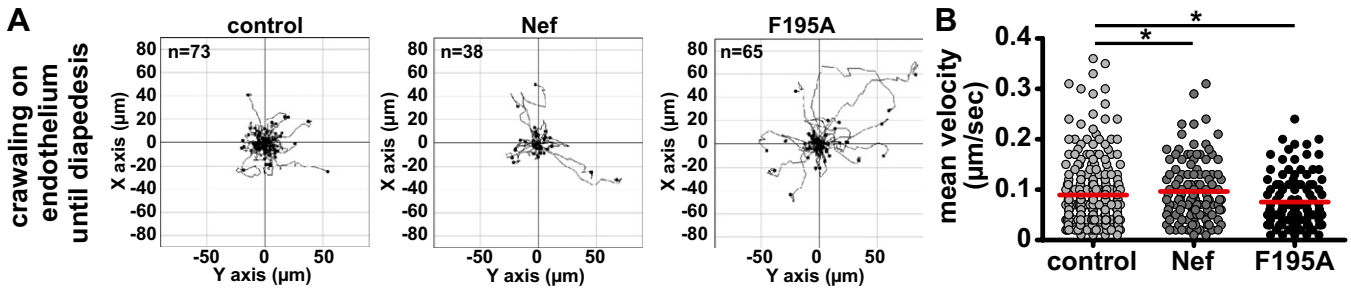

Fig. S6. Nef-expression does not exert pronounced effects on the locomotion of T lymphocytes on top of the endothelium. Transduced and sorted T lymphocytes were subjected to transendothelial migration (TEM) assays as in Fig. 2. (*A*) Single-cell tracks of cells crawling on top of the endothelium before successful diapedesis. The tracks are derived from one of four to five representative TEM experiments. Adhered T lymphocytes were tracked manually, starting when shear flow rates were first increased. (*B*) Mean velocity of single cells until successful diapedesis calculated from single cell tracks as shown in *A* from four to five independent TEM experiments. Red bars indicate mean values. *P* values have been calculated using a one-tailed ANOVA test with a Newman–Keuls posttest. $*P < 0.05$.

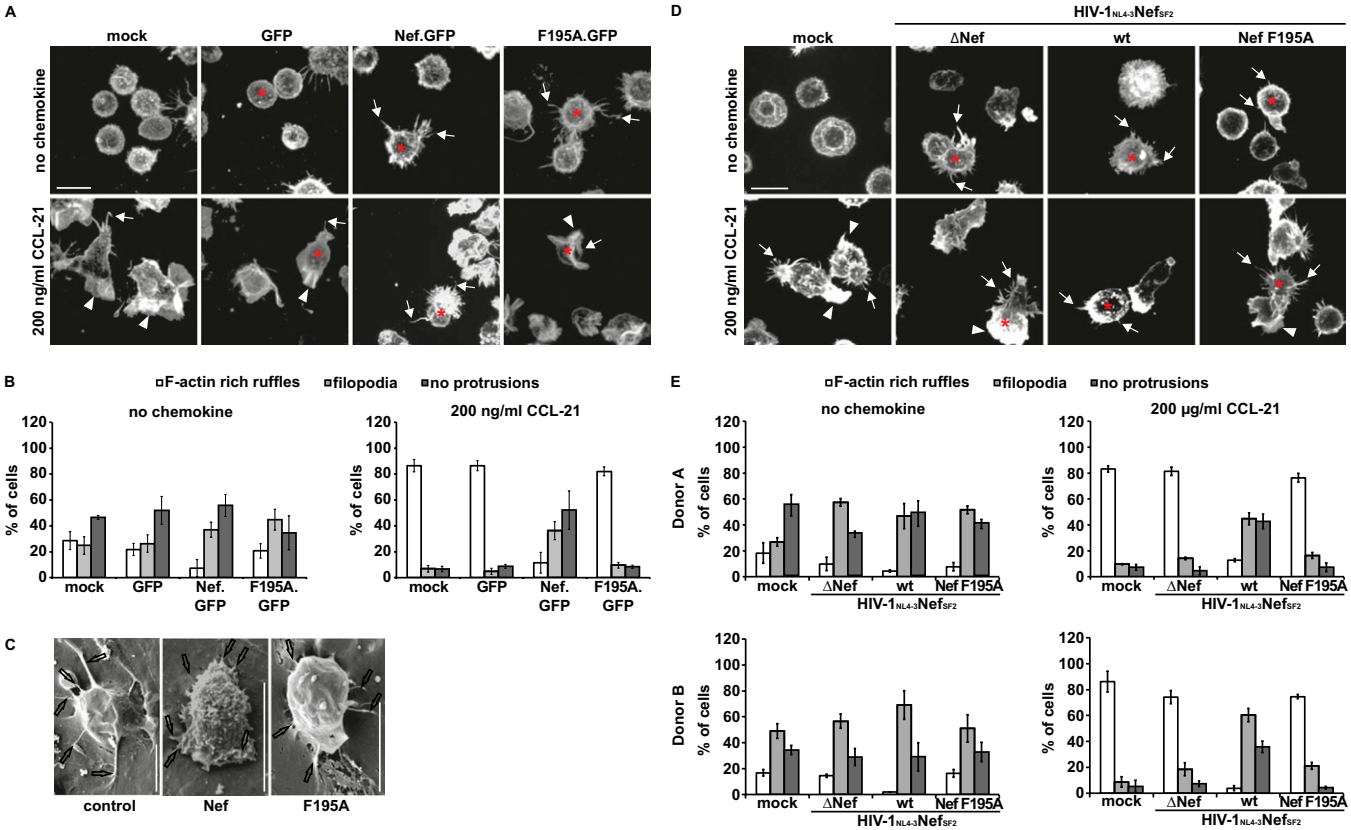

Fig. S7. Nef does not interfere with filopodia formation in transduced murine T lymphocytes and HIV infected human T lymphocytes. (*A*) Representative 3D maximum projections of confocal *z*-stacks of primary murine T lymphocytes transduced with the constructs shown in Fig. S2 for expression of GFP, Nef wt.GFP, NefF195A.GFP. Cells were plated onto poly-L-lysine–coated cover-glasses and analyzed for membrane ruffle and filopodia formation with and without stimulation by CCL-21. Cells were fixed and stained for F-actin. Red asterisks highlight transduced GFP^+ cells. Arrows and arrow heads indicate filopodia and F-actin rich membrane ruffles, respectively. (Scale bars, 10 µm.) (*B*) Quantification of the cells shown in *A*. Cells showing F-actin rich membrane ruffles or filopodia were quantified by manual counting of at least 100 transduced cells per condition. Cells showing showing F-actin–rich membrane ruffles and filopodia were counted as membrane ruffle-positive. Shown are mean values with SD of three independent samples. (*C*) Primary murine T lymphocytes were transduced and sorted as in Fig. S3 to achieve expression of Nef or NefF195A.GFP, and subjected to transendothelial migration as shown in Fig. 2. Five minutes after adherence to the endothelium, cells were fixed and processed for SEM. Shown are representative SEM pictures of T lymphocytes interacting with endothelial cells. Arrows indicate filopodial structures. (Scale bars, 10 µm.) Note that Nef does not suppress formation of filopodia but appears to induce the generation of numerous, microvilli-like short-cell protrusions in a F195-dependent manner. (*D*) Primary human lymphocytes were infected with HIV WT, a virus lacking Nef expression (HIVΔNef) or an isogenic virus encoding for NefF195A. Cells were stimulated with human CCL-21 identical to the murine lymphocytes shown in *A*. Shown are representative 3D maximum projections of confocal *z*-stacks. Red asterisks highlight HIV infected/CA^+ cells. Arrows point toward filopodia, arrow heads toward F-actin rich membrane ruffles. (Scale bars, 10 µm.) (*E*) Quantification of filopodia and F-actin–rich membrane ruffles of HIV-infected lymphocytes as in *B*. Shown are mean values with SD from triplicate infection of lymphocytes from two independent donors.

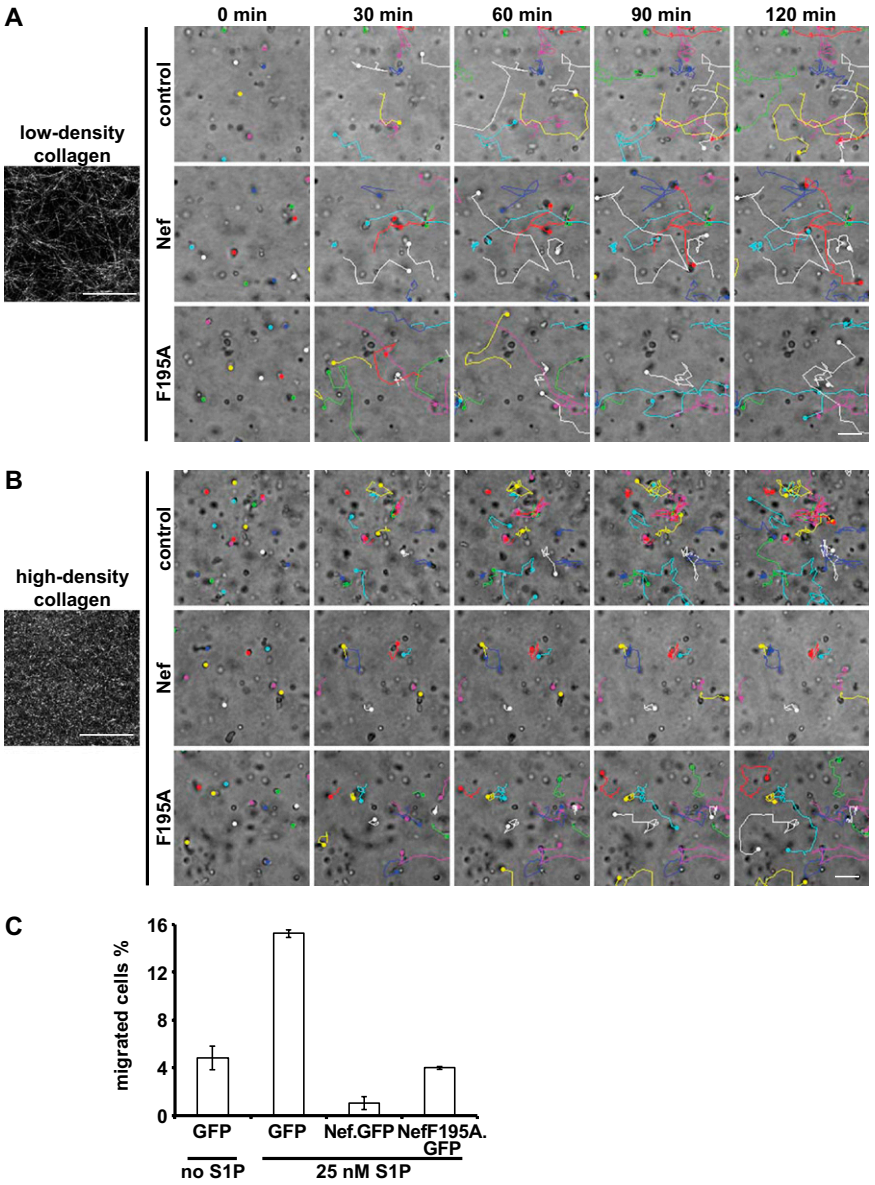

Fig. S8. Nef interferes with T-lymphocyte motility in 3D matrices dependent on the pore size. Shown are still images of additional time points of the 3D collagen migration assay shown in Fig. 4. (*A*) Low-density collagen (1.6 mg/mL) showing stills of Movie S3. (*B*) High-density collagen (4.6 mg/mL) showing stills of Movie S4. The panels on the left show the fibrillar structures of the collagen preparations used visualized as maximum projections of 10-μm stacks using confocal reflection microscopy. Moving cells are labeled with colored dots and their tracks are indicated over time. (Scale bars, 50 μm.) (*C*) Primary murine T lymphocytes were transduced with the constructs shown in Fig. S2 to achieve expression of GFP, Nef wt.GFP or NefF195A.GFP and subjected to transwell chemotaxis assays toward S1P using 5-μm pore transwell inserts. Shown is the absolute migration efficiency of GFP^+ cells as mean values with SD of one representative experiments performed in triplicates.

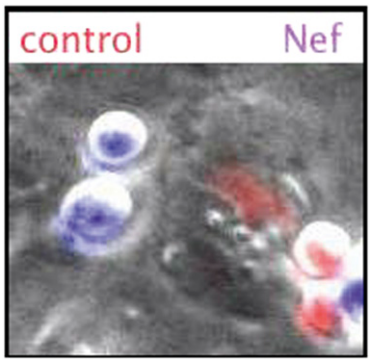

Movie S1. Nef interferes with transendothelial migration. Representative field of view of a TEM experiment. Shown is a TNF-α–stimulated, CCL-21–coated primary murine endothelial cell monolayer with control and Nef transduced T lymphocytes, labeled in red and blue, respectively. Cells were imaged over a time-course of 50 min with one image acquired/20 s. The movie starts when shear flow rates were first increased. Images were acquired using a 20× objective.

Movie S1

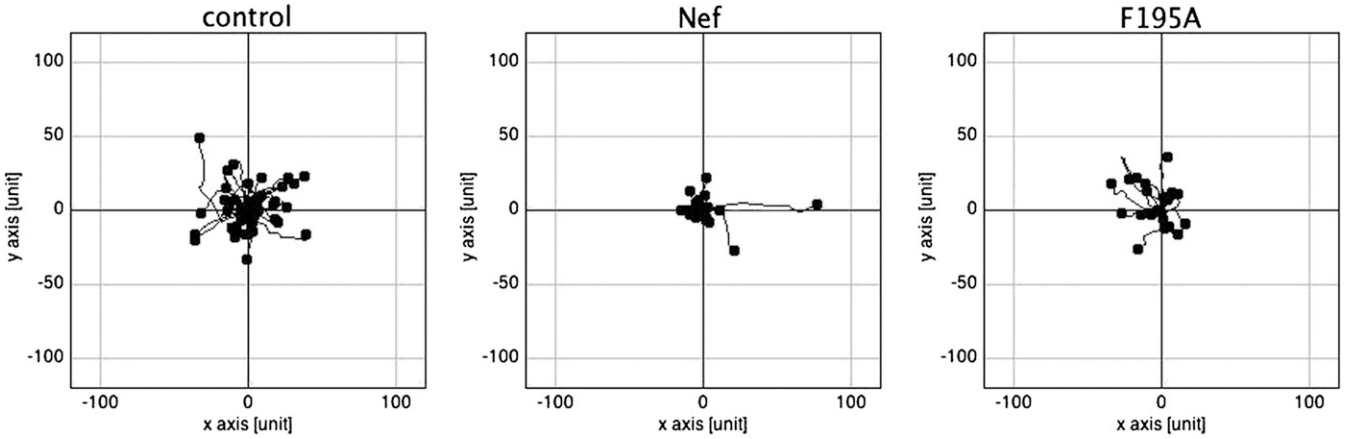

Movie S2. Single-cell tracks of T lymphocytes migrating underneath an endothelial cell monolayer. Control, WT Nef and Nef F195A transduced T lymphocytes were tracked following successful diapedesis while migrating underneath an endothelial cell monolayer until the end of the experiment. Different lengths of the tracks are result from diapedesis after different time points.

Movie S2

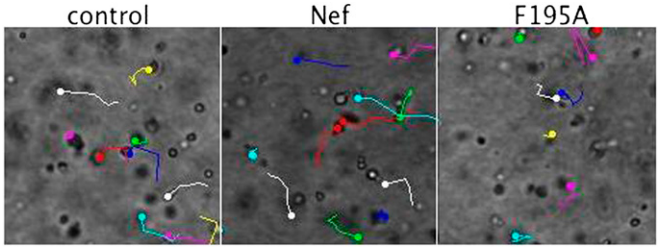

Movie S3. T lymphocytes migrating in low-density collagen matrices. Control, WT Nef and Nef F195A transduced T lymphocytes were embedded into low-density (1.6 mg/mL) collagen matrices in the presence of 100 ng/mL CCL-21. Migration of cells was monitored by bright-field microscopy over 2.5 h with one image acquired every 3 min. Moving cells are labeled with colored dots and their tracks are indicated over time. Images were acquired using a 10× objective.

Movie S3

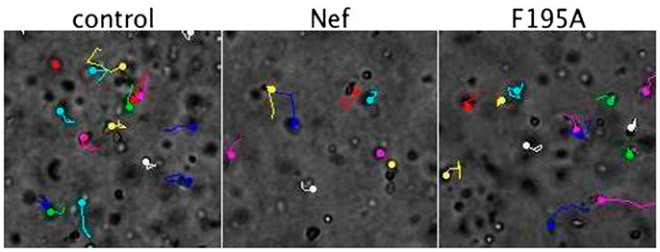

Movie S4. T lymphocytes migrating in high-density collagen matrices. Control, WT Nef and Nef F195A transduced T lymphocytes were embedded into high-density (4.6 mg/mL) collagen matrices in the presence of 100 ng/mL CCL-21. Migration of cells was monitored by bright-field microscopy over 2.5 h with one image acquired every 3 min. Moving cells are labeled with colored dots and their tracks are indicated over time. Images were acquired using a 10× objective.

Movie S4

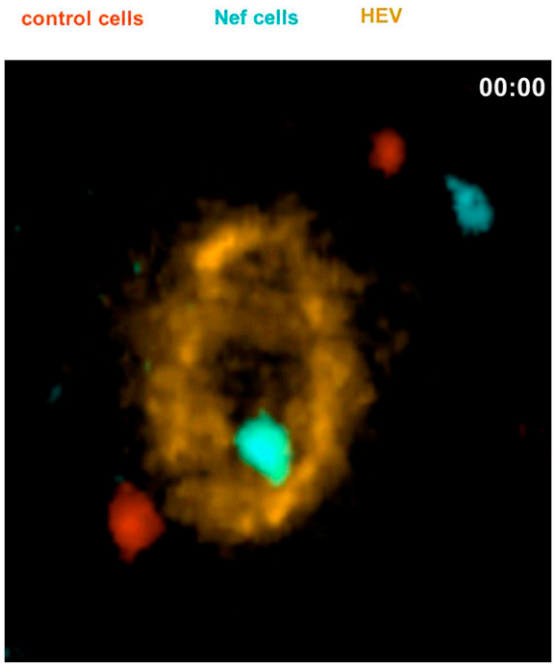

Movie S5. Nef interferes with diapedesis of T lymphocytes across HEVs in vivo. The 2PM intravital imaging of a surgically exposed popliteal lymph node 24 h postadoptive transfer of transduced, sorted, and CellTracker-labeled, T lymphocytes. Migration of cells close to a HEV was monitored over 20 min with one 3D stack acquired every 20 s. The HEV is labeled by injection of a fluorophor-coupled MECA-79 antibody and displayed in brown. Control cells are displayed in red, Nef-expressing cells in blue. Images were acquired using a 20× objective.

Movie S5

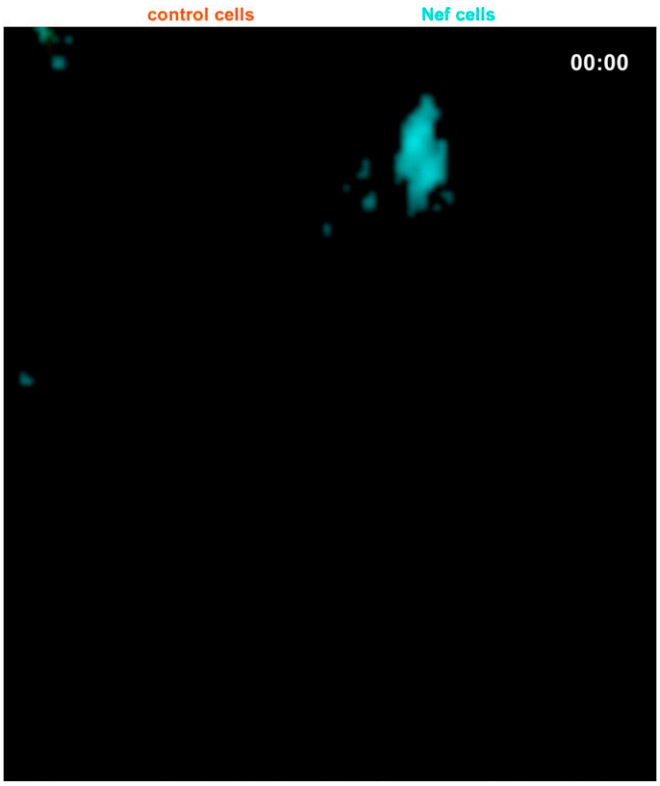

Movie S6. Nef reduces T-lymphocyte motility in vivo. The 2PM intravital imaging of a surgically exposed popliteal lymph node 24 h post adoptive transfer of transduced, sorted and CellTracker-labeled, T lymphocytes. Migration of cells in the lymph node parenchyma was monitored over 20 min with one 3D stack acquired every 20 s. Control cells are displayed in red, Nef-expressing cells in blue. Images were acquired using a 20× objective.

Movie S6